EFFECT OF SLIGHT LEADING EDGE BLUNTNESS ON FLAT PLATE HEAT TRANSFER AND BOUNDARY LAYER TRANSITION AT HYPERSONIC MACH NUMBERS

Koichi Hozumi, Shinji Nagai, Keisuke Fujii
Akira Yoshizawa and Nobutoshi Hara

Aerodynamics Division
National Aerospace Laboratory
7-44-1 Jindaiji-Higashichou Chofu, Tokyo 182 Japan

Abstract

To obtain a prediction method of a heating rate on the wing of HST, the effect of wing leading-edge bluntness on the heat transfer distribution has been investigated. Heat transfer rates over flat plates with slight leading edge bluntness were measured in the NAL 50-cm hypersonic wind tunnel using an infrared (IR) scanning system. The position of the boundary layer transition on the wing surface were measured at the same time to investigate the slight nose bluntness effect on the transition.

The results of the present studies show that leading-edge bluntness has pronounced effect on the heat transfer near the leading edge of the plates. Good predictions for the heat transfer rate at the leading-edge region were obtained by a local similar boundary layer analysis based on the boundary-layer edge condition determined by both the total pressure behind the leading edge normal shock wave and the surface pressure. The transition data observed in the present tests showed that the local boundary layer conditions based on the leading-edge normal shock wave loss are also an important parameter for the onset of boundary layer transitions.

1. Introduction

In developing the future hypersonic transport, a configuration with a sharp nose and wing leading-edge is essential to obtain high L/D ratio aerodynamic characteristics[1]. Experimental studies on the aerothermal problems associated with hypersonic flight of such HST were conducted at NAL hypersonic wind tunnel[2]. These studies showed that the heating rate on the vehicle is unexpectedly severe near the leading-edge region of the wing with slight leading-edge bluntness. In order to obtain a prediction method of such heating rate on the wing, the effect of wing leading-edge bluntness on the heat transfer distribution has been investigated.

Several experimental investigations have been made on the effect of leading-edge bluntness on local heat transfer[3,4,5,11]. A reduction of heat transfer in significant downstream of nose region caused by entropy layer swallowing effects[3,4] was investigated by Ferri et.al.. However, the nose bluntness effect on heat transfer in near the leading-edge region was not examined precisely, although many experimental results showed somewhat higher heat transfer rate than the theoretical prediction[5].

In the present investigation, heat transfer rates over flat plates with slightly blunted leading-edge were measured at NAL hypersonic wind tunnel using infrared cameras. An analysis to explain the reason of higher heating rate at leading-edge region was made for the NAL data. The position of the boundary layer transition on the wing surface was measured at the same time to investigate slight nose bluntness effect on the transition, as the prediction of position of the boundary layer transition is also important for the aerothermal design of HST because of its increasing nature of heat transfer distribution.

2. Apparatus and Model Description

2.1 The Wind Tunnel and Test Conditions

The tests were conducted in the NAL 50cm hypersonic wind tunnel at Mach numbers of 5.05, 7.1, and 12.0 and at angles of attack α between 0° and 10°. The Reynolds number range tested was about 3.5 to 9 million per meter. The variable sweep tests were also conducted to investigate heating rate of leading edge with sweep angle Λ. The test conditions of the present flat plate models are shown in Table 1. Further details of the tunnel and its operating characteristics are given in Reference 6.

2.2 Models

The configuration of flat plate models, ground finished flat plate model of machinable ceramics (Macol type p) with thickness of 10.0 mm for the flat parallel part is shown in Fig.1. Two different leading-edge cross-section with thickness of 0.3mm (type I leading edge) and 0.75mm (type II leading-edge) at edge were tested at Mach numbers of 5.05 and 12.0, and 7.1, respectively. The leading-edge sweep of this model could be varied in axis near the center of the model; thus, the model had five different wing sweep angles: Λ = 27°, 40°, 55°, 70°, and 83°. A cylindrical leading-edge model with 3mm thickness (Type III leading edge) was also tested at a Mach number of 7.1 to

obtain boundary layer transitions data without the nose contamination effect[2].

3. Test Procedure and Instrumentation

3.1 Heat Transfer Measurements Technique

The Infrared Scanner: Thermal mapping of heating patterns induced on wind tunnel models by convective heating was obtained using a commercially available infrared (IR) scanning system. Two IR video system of 4 and 8 bit temperature resolution with 256 x 100 pixels and scanning speed of 30 frame/sec and 100 frame/sec, respectively, were used. The infrared imaging system was positioned inside of the test section, above and below the main free-jet to obtain data of leeward and windward data at the same time.

Model Setup: The models were sting-supported in the test section of the tunnel and were injected in a few tenths of a second at a pre-set angle of attack by means of an air-cylinder high speed ejection system. To determine model ejection time and initial time of heating (t=0), three trigger pulse at position of start of ejection, nozzle boundary layer edge, and center of wind tunnel were used.

The Digital Image Processing System: The data was recorded in digital form on cassette tape. Processing the data from tape and the reduction of aerodynamic heating was done in off-line mode transferring the digitized temperature data of the IR image record to the NAL computing system.

3.2 Heat Transfer Data Reduction

Data Reduction Method: The heat transfer distributions on the flat plates are obtained by the Jones-Hunt[7] method using time history of surface temperature on the model obtained from IR image data.

Solution of the equation governing the one-dimensional transient conduction of heat into solid of known thermal properties, with appropriate boundary conditions, results in the expression used to reduce IR camera data:

$$h = \sqrt{\rho c_p k / t}\ \beta \qquad (1)$$

where

$$\frac{T - T_i}{T_{aw} - T_i} = 1 - e^{\beta^2}\,\mathrm{erf}(\beta) \qquad (2)$$

In eqs.(1) and (2), ρ, c_p and k are density, specific heat and thermal conductivity of model material, respectively, and T_i and T_{aw} are initial temperature of model and adiabatic wall temperature, respectively. From this relation, if time history of surface temperature T is known, heat transfer coefficient h is able to be obtained for a time t.

Accuracy analysis: Factors affecting data accuracy significantly were carefully examined. The model emittance was experimentally determined by uniformly heating to a known temperature which was simultaneously measured with thermocouple, and measuring the radiant emittance in the IR image. Emissivity of black paint coated Macol Type P was measured to be 0.95 (the emissivity without coating is 0.74) for the temperature range of present test.

Determination of model outline edge were carefully determined from initial image outline of models just before the start of test and false high temperature illumination region around the edge of model was removed.

Difference in initial temperature T_i affects the data accuracy significantly. Initial temperature of model was measured from the thermocouple output on the model and initial image of IR camera by setting temperature measurement range of camera as high sensitivity temperature resolution. Control of the model initial temperature was not done.

When the model is ejected into main stream, the model initially receives heating by free-jet shear layer which has different level of flow enthalpy than the main stream. This initial disturbance of heating has large effect on the reduced data results for case of short measuring time tests. Based on the constant heat transfer coefficients assumption in the Jones-Hunt method, the virtual starting time of step heating was determined extrapolating linear relation t β^2 in eq.(1) as shown in Fig.2. To check the adequacy of the estimated virtual starting time of heating, comparison of both heat flux obtained by Jones-Hunt method and Cook-Felderman method[8] from the time history of surface temperature of a point near the leading edge was made.

4. Results and Discussion

4-1. Hypersonic Flow Past a Flat Plate with Slightly Blunted Leading Edge.

Hypersonic flow past a flat plate with a slightly blunted leading edge is affected by two distinctive effects, i.e., the effect caused by hypersonic viscous interaction near a sharp leading edge and the nose bluntness effects. Viscous interaction may be defined as the mutual interaction between the external flow field and the boundary layer growth around a body of given shape. Furthermore, blunt leading-edge thickness gives a flow the entropy rise across the shock wave. Nose bluntness gives the following three effects, effects of reduction of local Reynolds number, induced pressure by nose bluntness, and subsequent entropy layer swallowing.

Characteristics of flow past a leading edge of slightly blunted thin body is complicated by the fact that the viscous interaction and the nose bluntness effects exist at the same time and the pressure on the surface is not uniquely determined by the effective body geometry. In spite of such fact, an approximate

surface pressure distribution could be predicted satisfactory by a combination of pressure distribution from shock-wave boundary layer interaction theory and blast wave theory. The pressure distribution given by theory of viscous interaction[9] are usable with combination of inviscid pressure distribution. And numerous works are available on the prediction of the inviscid pressure distribution over a blunt-nosed plate in hypersonic flow, including correlations of solutions obtained by the method of characteristics and various blast wave analogy solutions as reviewed by Lukasiewicz[10].

4-2 Leading-Edge Shock Wave Effects on Heat Transfer

Available theoretical methods are adequate for prediction of pressure distribution on a blunt-nosed flat plate as above mentioned: however, the measured heat transfer distribution at the leading-edge region are always somewhat higher than the theory based on free-stream flow condition as shown by the present data in the following section 4-3. To make clear the reason of this higher heating rate, an analysis based on local flow condition determined by the total pressure behind bow shock wave p_{02} and model surface pressure p_w was attempted.

The character of hypersonic flow past a leading edge of a semi-infinite flat plate with slight bluntness is sketched in Fig.3. The total pressure along the boundary layer edge is lower than the total pressure in the free stream ahead of bow shock wave. An assumption that near the leading edge the local total pressure is reduced to the value of total pressure behind the leading-edge normal shock wave was made. The viscosity μ was assumed to vary as power of absolute temperature ($\mu \sim (T)^{\omega}$, $\omega=0.5$).

Then, the local Mach number at boundary layer edge M_e is specified by the local static and total pressures. The ratio of Reynolds number based on free-stream and local boundary layer edge condition are also obtained using the above described assumptions[11]. The local unit Reynolds number Rex_L was found to be lower than free-stream unit Reynolds number Re_∞, and to have negligible dependence on leading-edge bluntness within the undermentioned distance x_s. This reduction depends on the square root of the ratio of total pressures across the normal bow shock wave. Fig.4 shows the effect of normal shock wave on the ratio of Reynolds number Rex_L/Re_∞.

The length along a flat plate where total pressure at boundary layer edge is p_{02} condition (x_s in Fig.3) was examined. The relation of mass flow through the boundary layer on a flat plate and the mass flow through the normal shock wave portion of leading-edge bow shock wave (assumed equal to nose bluntness d) is

$$(\rho_\infty u_\infty)d/2 = \int_\delta^0 \rho u dy \qquad (3)$$

The theoretical prediction of boundary-layer thickness on a flat plate[11] is

$$\delta/d=[1.73/M^3(T_w/T_\infty)+0.332(\gamma-1)+ 4.27/M^2]\ ((M^2C_w/Red)\ x/d \qquad (4)$$

From eq.(3) with combination of flat plate boundary layer profile[12] and eq.(4), the length of x_s is calculated for an assumed weak interaction pressure distribution. Fig.5 shows that x_s is remarkably large and it is reasonable to assume that total pressure in the leading-edge region is p_{02} at boundary-layer edge.

4-3 Heat Transfer Measurements Results

Heat Transfer Based on Free Stream Condition

Examples of centerline heat transfer distribution at Mach numbers of 5.05, 7.1 and 12.0 at $t \fallingdotseq 0.1$ sec are presented in Fig.6-1, 2, 3 in form of Stanton number St_∞ based on free-stream condition. Heat transfer rate calculations on flat plate based on laminar boundary layer theory[13] and strong interaction theory[9] are also plotted for comparison. The magnitude of measured Stanton number on the centerline were much larger than the corresponding theoretical two-dimensional laminar plate value at the leading-edge region ($x \leq$ 20mm).

Heat Transfer Based on Local Flow Condition

Correlation of flat plate heating data representing by local Stanton number ST_L were examined. The present and available experimental Stanton number St_L for the Reynolds number based on the local boundary layer edge condition Rex_m is shown in Fig.7 ,8 and 9.

As shown in Fig.7, good predictions for the heat transfer rate at the leading edge region were obtained by a local similar boundary layer analysis based on the boundary layer edge condition determined by the total pressure behind the leading edge normal shock wave p_{02} and the surface pressure p_w.

To confirm the validity of the above mentioned analysis, correlation of other available heat transfer data was also done in case of $\Lambda=0°$ and $\Lambda \neq 0°$ as shown in Fig.8 and 9, respectively. Fig.7,8 and 9 shows that effect of Mach Number, angle of attack and the sweep angle on heat transfer data past flat plate could correlate by a single flat plate relation eq.(5) based on local boundary layer edge condition.

$$St_L = 0.413/Rex_m \qquad (5)$$

Analysis in previous section 4-2 shows that leading-edge region is the region of reduced Mach number and Reynolds number near the surface (at boundary layer edge). The distance from leading edge along flat plate surface x_s where total pressure at the outer edge of

boundary layer remains p_{02} condition is considerably long as shown in Fig.5. These analytical and experimental results show that the higher heat transfer at leading-edge region is due to above mentioned reduced Reynolds number resulting from the leading-edge normal-shock wave loss.

4-4. Transition Observation in the Present Test

Transition observation by the IR camera in the present tests showed that there was a clear dependence of onset of transition on angle of attack α and sweep angle Λ . And leading-edge contamination was observed to have a large effect[2].

Fig.10 shows relation between transition Reynolds numbers based on free stream condition Rex_t and free stream Mach number M_∞ for the present observations. Although Fig.10 do not show good correlation, clear tendencies of transition were observed in the present tests. Rex_t increases as M_∞ increases. Rex_t decreases as Λ and α increases. These tendencies agree with those of the other accepted experimental results.

4-5 Correlation of Transition Reynolds Number

Predicting boundary layer transition remains a critical problem in supersonic and hypersonic flows. This phenomenon has a large impact on many aspects of high speed vehicle design, not only because of its effects on skin friction drag and surface heat transfer rates, but also on engine inlet flow characteristics. It is accepted that the onset of boundary layer turbulence is the results of instability waves which originate in laminar boundary layer. However, there are many factors affecting onset of boundary layer transition.

Transition in Wind Tunnel Tests

The problem of transition studies in wind tunnels is that the free stream noise affects transition. In supersonic and hypersonic flows, the main factor affecting transition is also noise. The origin of noise lies in the pressure disturbances radiated from turbulent boundary layer developing along the wind tunnel walls.

In case of constant free-stream Mach number and temperature ratio T_w/T_{aw}, the transition Reynolds number increases with increasing unit Reynolds number u_e/υ_e and increasing wind tunnel size. This empirical relation lead to the following expression: $Rex_t \sim (u_e/\upsilon_e)^{0.5}\, f(p)$, f increases as the test section circumference increases.

The effect of tunnel size was first demonstrated by Pate and Schueler[14]. Their extensive study on the correlation of Rex_t with radiated noise in supersonic flow showed that the increase in Rex_t with the unit Reynolds number in supersonic and hypersonic wind tunnel is directly related to the radiated aerodynamic noise emanating from the tunnel wall turbulent boundary layer.

Correlation of Flat Plate Boundary Layer Transitions

Experimental studies[15-21] showed that increase in small nose-tip bluntness increased the critical (transition onset) Reynolds number significantly. The predictions also show that increase in nose bluntness delays transition. In the present studies, an attempt to obtain a correlation by integrating the effects of various factor affecting transition, such as wall cooling or nose bluntness was done.

To know the Mach number effect on transition separately, flat-plate transition data of a tunnel should be plotted for a constant free-stream unit Reynolds number since this is the case where the radiated aerodynamic noise is constant. As unit Reynolds number are constant in the present test at Mach numbers of 5.05 and 7.1, the unit Reynolds number effects can be removed and the Mach number effect was examined separately.

The present transition data showed that analysis of the transition onset using the local boundary layer edge conditions calculated from the leading-edge normal shock loss are also important. Relation between Mach number at boundary layer edge based on local flow condition Me, main stream Mach number at outside of boundary layer Md, and transition Reynolds number based on local flow condition (obtained in the same way as in section 4.2) Rex_L was analyzed. Good correlation of the present transition data using these local flow properties was obtained as shown in Fig.11.

Nose-Bluntness Reynolds Number and Boundary Layer Thickness Effects on Transition

Correlation of other available flat plate transition data were also performed. Correlation curves for the present and other available flat plate transition data[15-19] showed that onset of transition for slight blunt nosed plates are related to not only the local Mach number at boundary layer edge M_e but also the nose bluntness Reynolds number Red_∞ .

Based on these results, an attempt to obtain more general correlation was made. Fig.12 and 13 shows relation between nose-bluntness Reynolds number Red_∞ and local boundary layer thickness to nose bluntness ratio at transition location $(\delta/d)_{tr}$.

The flow past the flat plate with blunt leading edge will have following two important features; shape of shock wave and boundary layer developing on the flat plate. Shape of shock wave is associated with outer entropy layer and boundary layer is viscous flow near the wall. Therefore, two y direction scales, boundary layer and entropy layer thicknesses determine total flow field. The thickness of entropy layer is related

to the nose bluntness d. Thus, two characteristics length for the flow field δ and d can be selected as viscous and inviscid characteristic lengths, respectively. Consequently, the ratio of the both length δ/d is important parameter to show the degree of inviscid and viscous effect on the flow field. And the ratio at x_S, $(\delta/d)_S$, represent some standard combined x and y direction scale ratio for the flow field.

Fig.12 and 13 shows the relation $(\delta/d)_{tr} = C*Red_\infty{}^n$ and the average slope of this correlation n is about -0.82. Correlation curve for lower noise and higher Mach number free stream moves toward right hand side in the figures. And at location of about $10*(\delta/d)_S$ sudden change of correlation curve (increase in $(\delta/d)_{tr}$) was shown.

These results show that Red_∞ and $(\delta/d)_{tr}$ at transition onset are dominant parameters for the onset of supersonic and hypersonic transition. These observed results will be related to some fundamental mechanism of onset of transition in compressible flow showing that local flow condition have large effects on transition as well as upstream history of flow affected by free stream disturbances.

5. Conclusions

In the present experimental studies, to make clear the heating mechanism for sharp leading edge of HST, an investigation on the effect of flat plate leading-edge bluntness on the heat transfer distribution and transition was done.

Heat transfer measurement at leading-edge region indicated the following conclusions.

1) Heat transfer coefficient is higher than the theoretical value based on the free-stream flow condition.
2) Boundary layer edge condition of flow past leading edge can be determined by the total pressure behind normal-shock portion of leading-edge shock wave p_{02} and surface pressure p_w assuming that flow is expanded isentropically from bow shock wave.
3) Relation between heat transfer data and Reynolds number based on above mentioned local flow condition agrees well with the theoretical flat plate relation. This held true for many available heat transfer data at low to moderate hypersonic flow.

The transition data analysis showed following conclusions.

1) Transitions which occur far behind the leading edge are also related to the local flow conditions determined by p_{02} and p_w.
2) Transition Reynolds number based on local boundary layer edge condition Rex_L increases with increasing local Mach number Me and decreases with increasing main stream Mach number Md.
3) Various available flat plate transition data at supersonic and hypersonic flow showed that for one wind tunnel a general correlation curve between nose bluntness and boundary layer thickness ratio $(\delta/d)_{tr}$ and nose bluntness Reynolds number based on free stream condition Red_∞ was obtained.

These results help explain the bluntness effect on heat transfer and transition, and also help in aerothermal designing of HST with slender and slightly blunted wings at hypersonic cruise conditions.

6. References

1) Aihara,Y., Morishita,E., Okunuki,T., Nomura,S., and Hozumi,K., "Experimental Study on Drag Reduction of Hypersonic Transport Configuration" ICAS-90-3.10.1 (1990)
2) Hozumi,K., Nomura,S., Aihara,Y., Morishita,E., and Okunuki,T., "Experimental Investigation of Aerothermal Problems Associated with Hypersonic Flight of HST," ICAS-92-4.9.3 (1992)
3) Ferri,A., "Some Heat Transfer Problems in Hypersonic Flow," Aeronautics and Astronautics, p349-377, Pergamon Press (1960).
4) Rotta,N.R., and Zakkay,V., "Effect of Nose Bluntness on the Boundary Layer Characteristics of Conical Bodies at Hypersonic Speeds," Astronautica Acta, Vol.13, p.507-516.
5) Harvey, W.D., "Effect of Leading-Edge Bluntness on Pressure and Heat Transfer Measurements over a Flat Plate at Mach Number of 20," NASA TN D-2846, October 1965.
6) Hiraki,I., et.al., " Design and Construction of the 50cm Hypersonic Wind Tunnel at National Aerospace Laboratory," NAL TR-116, Sep. 1966.
7) Jones,R.A., and Hunt,J.L., "Use of Fusible Temperature Indicators for Obtaining Quantitative Aerodynamic Heat-Transfer Data," NASA TR R-230, Feb., 1966.
8) Cook,W.J., and Felderman,E.J., "Reduction of Data from Thin-Film Heat Transfer Gauge: A Concise Numerical Technique," AIAA J., Vol.4,No.3, March, 1966.
9) Hayes,W.D., and Probstein,R.F.,"Hypersonic Flow Theory," Applied Mathematics and Mechanics 5, Academic Press, 1959.
10) Lukasiewicz,J., "Blast-Hypersonic Flow Analogy Theory and Application," ARS Journal, p1341-1346 September 1962.
11) Creager,M.O., "Effects of Leading-Edge Blunting on the Local Heat Transfer and Pressure Distributions over Flat Plates in Supersonic Flow," NASA TN-4142, Dec., 1957.
12) Willson,R.E., "Laminar Boundary-Layer Growth on Slightly Blunted Cones at Hypersonic Speeds," J. Spacecraft, Vol.2., No.4, July-Aug., 1965.
13) Van Driest, E.R., "Investigation of Laminar Boundary Layers in Compressive Fluids Using the Crocco Method,"

NACA Technical Note 2597, Jan. 1952.
14)Pate, S.R., and Schueler, C.J., " An Investigation of Radiated Aerodynamic Noise Effects on Boundary-Layer Transition in Supersonic and Hypersonic Wind Tunnels," AIAA Paper No.68-375, April 1968.
15)Jillie,D.W., and Hopkins,E.J., "Effects of Mach Number, Leading-edge Bluntness, and Sweep on Boundary-Layer Transition on a Flat Plate," NASA TN D-1071, September 1961.
16)Chen,F.J., and Malik,M.R., "Comparison of Boundary Layer Transition on a Cone and Flat Plate at Mach 3.5," AIAA Paper No. AIAA-88-0411, January, 1988.
17)Stetson,K.F.,Thompson E.R., Donaldoson, J.C.,and Siler,E.R., "Laminar Boundary Layer Stability Experiments on a Cone at Mach 8. Part2 : Blunt Cone," AIAA Paper No.83-1761 (1983).
18)Potter, J.L., and Whitfield,J.D., "Effect of Slight Nose Bluntness on Boundary Layer Transition in Supersonic Flows," J. Fluid Mech., Vol.12, Part 4, pp.501-535, 1962
19)Softly, E.J., Graber,B.C., and Zempel, R.C., "Experimental Observation of Transition of the Hypersonic Boundary Layer," AIAA J., Vol.7, No.2, pp.257-263, 1969.

Table 1 Experimental conditions

M	P0 (bar)	T0 (°K)	Re/m($\times 10^{-7}$)	α (deg)	Λ (deg)
5.05	8.2	560 - 580	0.8 - 0.83	0 10	0, 27,40 55,70,83
7.10	29.8	760 -800	0.78 - 0.9	0 10	0, 40 55,70
12.0	88.6	1115	0.366 - 0.375	0	0 10

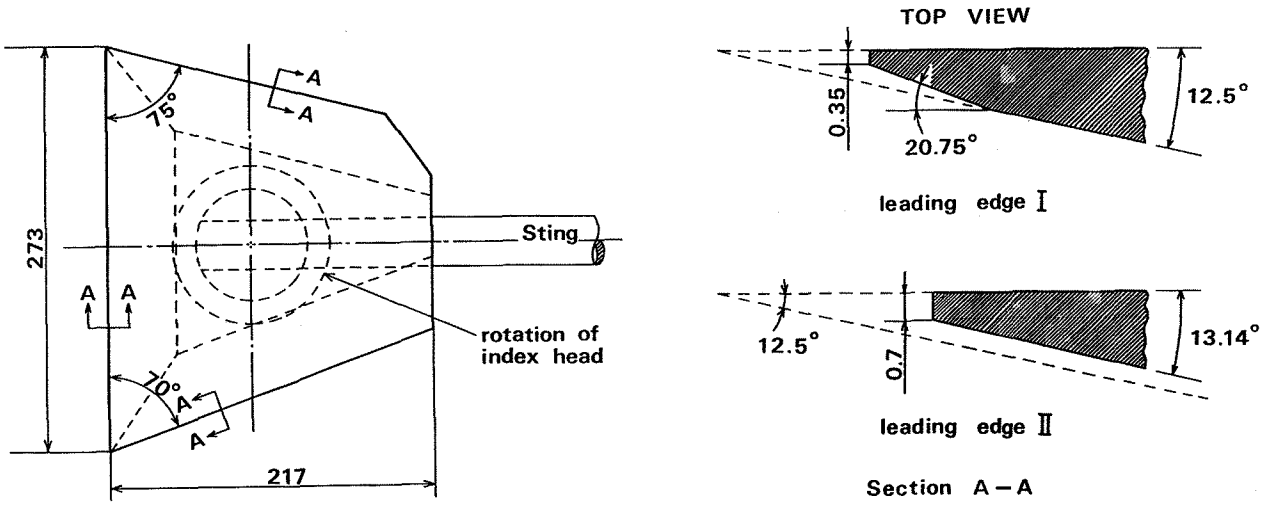

Fig.1 Flat plate models

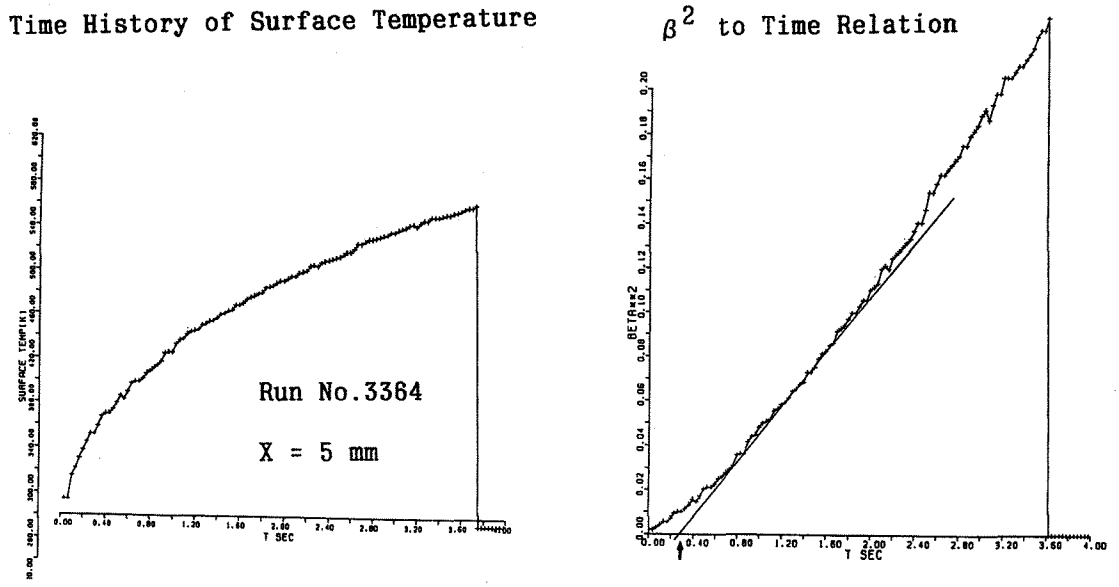

Fig.2 Estimation of virtual starting time of heating

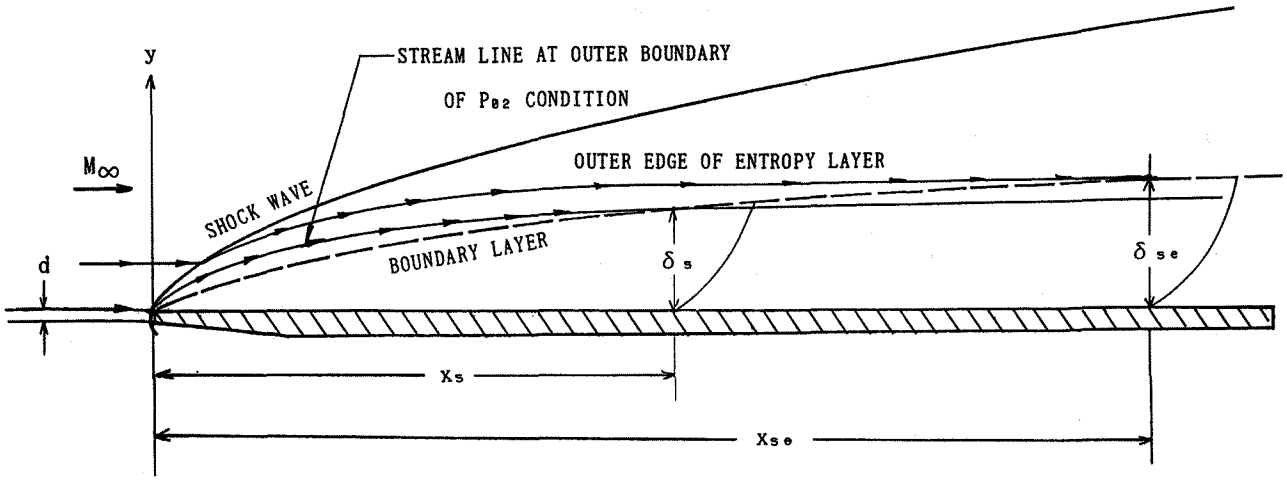

Fig.3 Hypersonic flow past a flat plate with slightly blunted leading edge

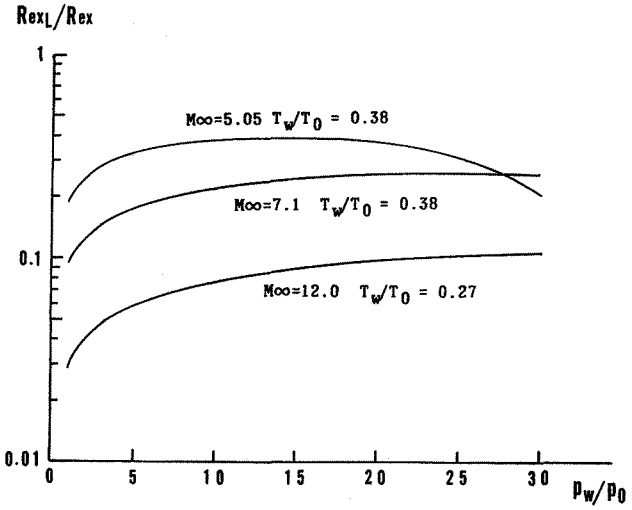

Fig.4 Effect of normal shock wave on local Reynolds number

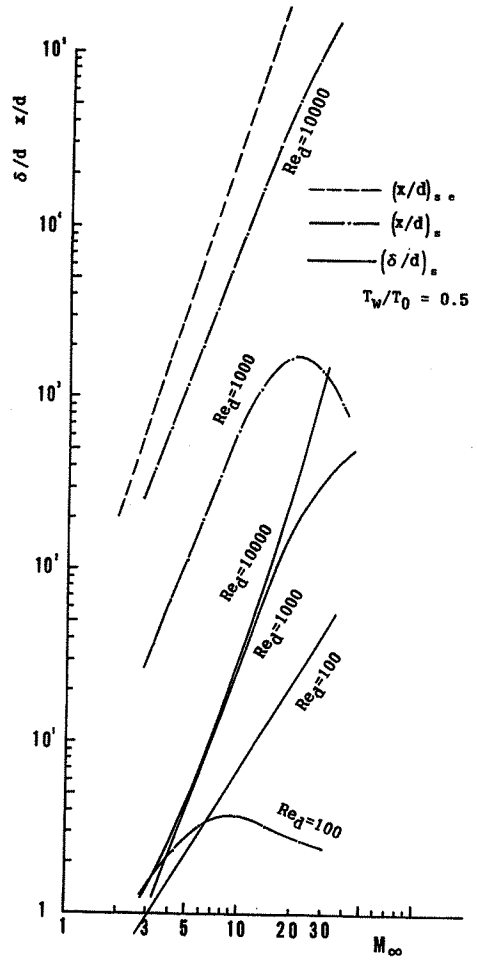

Fig.5 Extent of p_{02} condition at boundary-layer edge

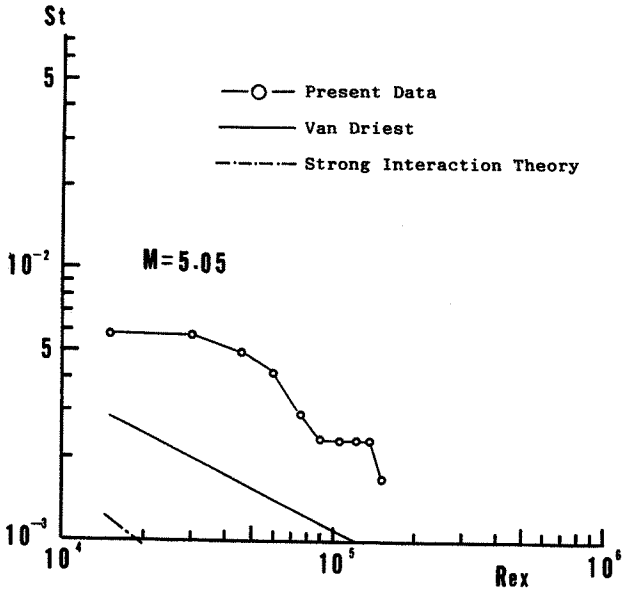

Fig.6-1 Heat transfer distribution along centerline of flat plate
(M=5.05, α =0°, Λ= 0°, t= 0.1339 sec)

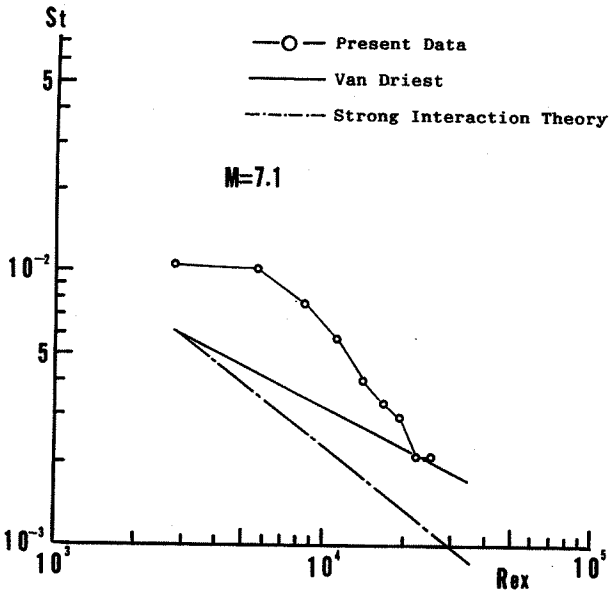

Fig.6-2 Heat transfer distribution along centerline of flat plate
(M=7.1, α =0°, Λ = 0°, t=0.0664 sec)

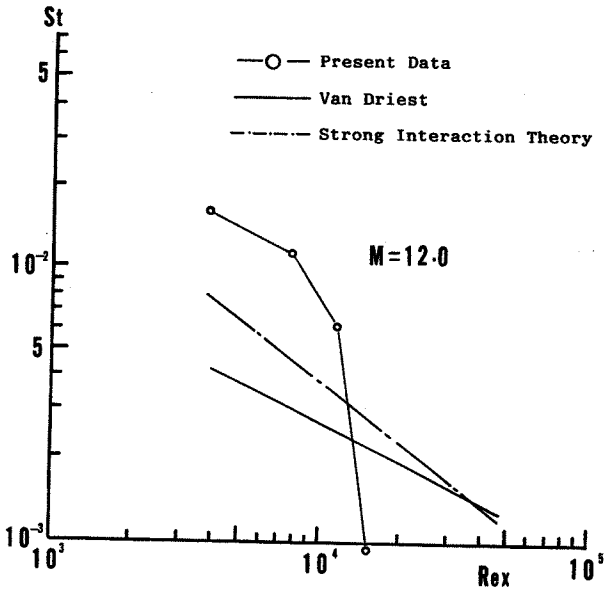

Fig.6-3 Heat transfer distribution along centerline of flat plate
(M=12.0, α =0°, Λ = 0°, t=0.0664sec)

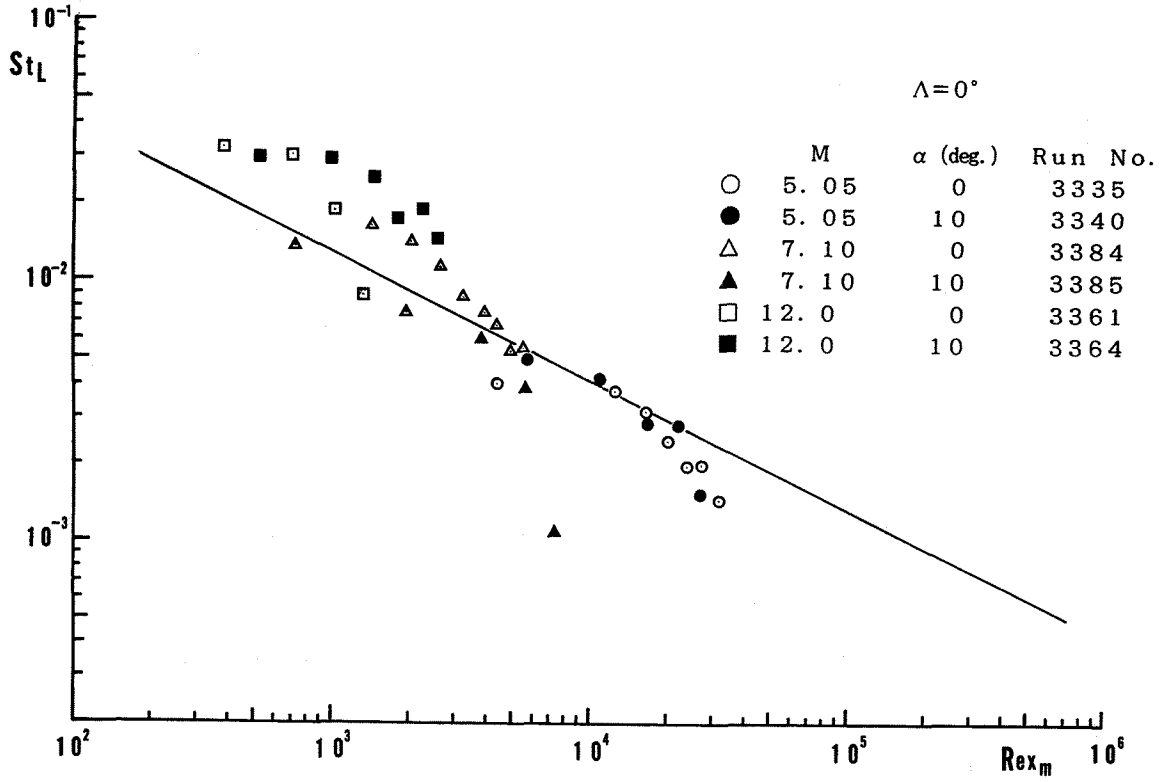

Fig.7 Variation of Stanton number with Reynolds number based on local flow conditions ($\Lambda=0°$, present data)

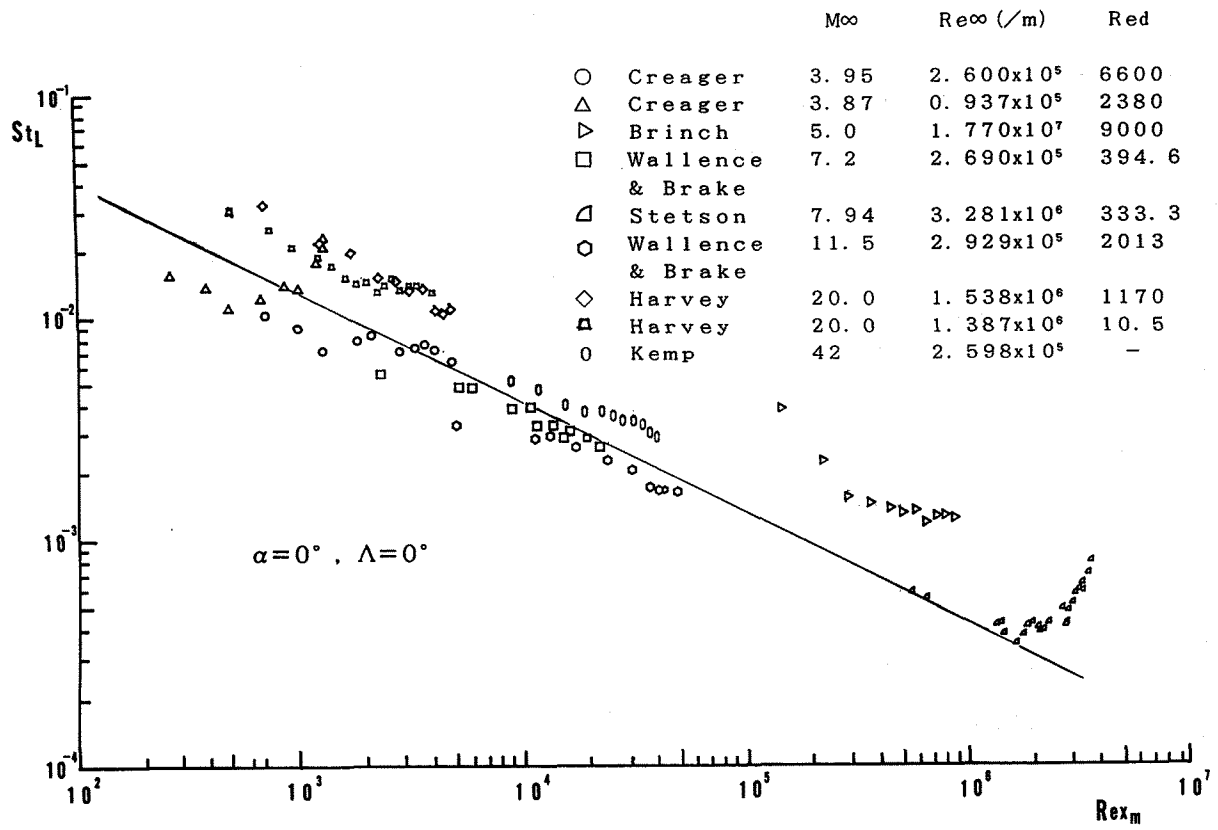

Fig.8 Variation of Stanton number with Reynolds number based on local flow conditions ($\Lambda=0°$, other available data)

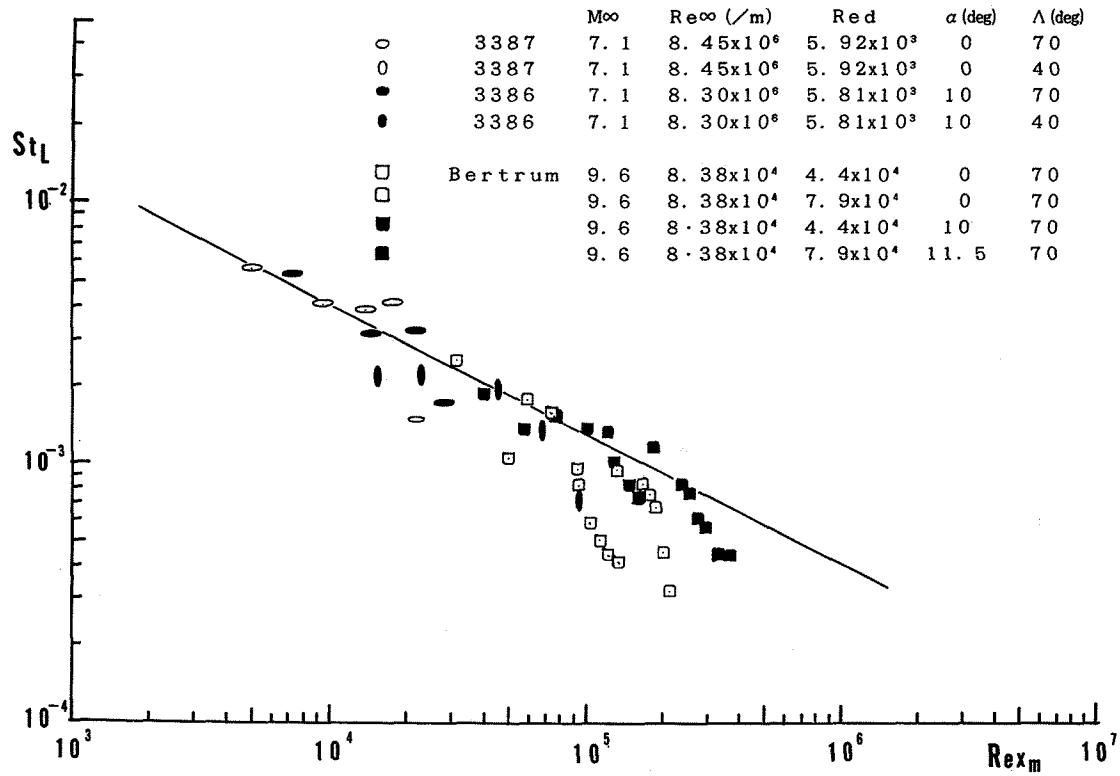

Fig.9 Variation of Stanton number with Reynolds number based on local flow conditions
(Λ ≠ 0°, present and existing data)

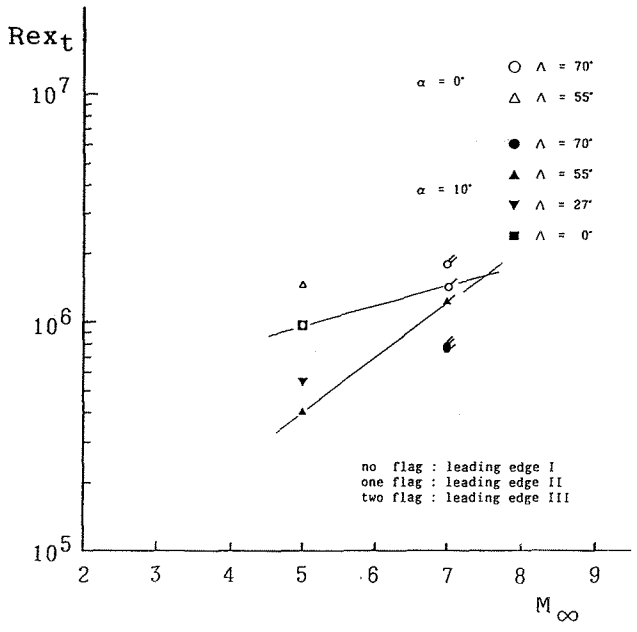

Fig.10 Observed transition Reynolds number at the present test.
(Rex_t M_∞)

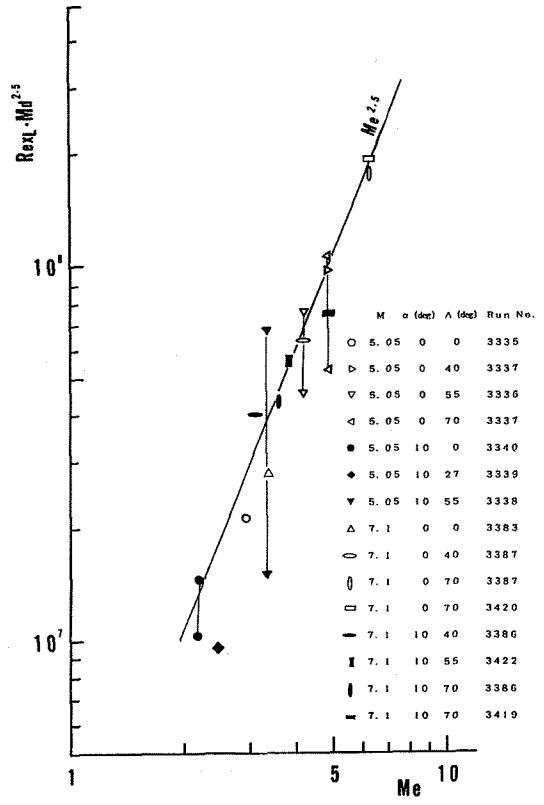

Fig.11 Correlation of transition data (present test data)

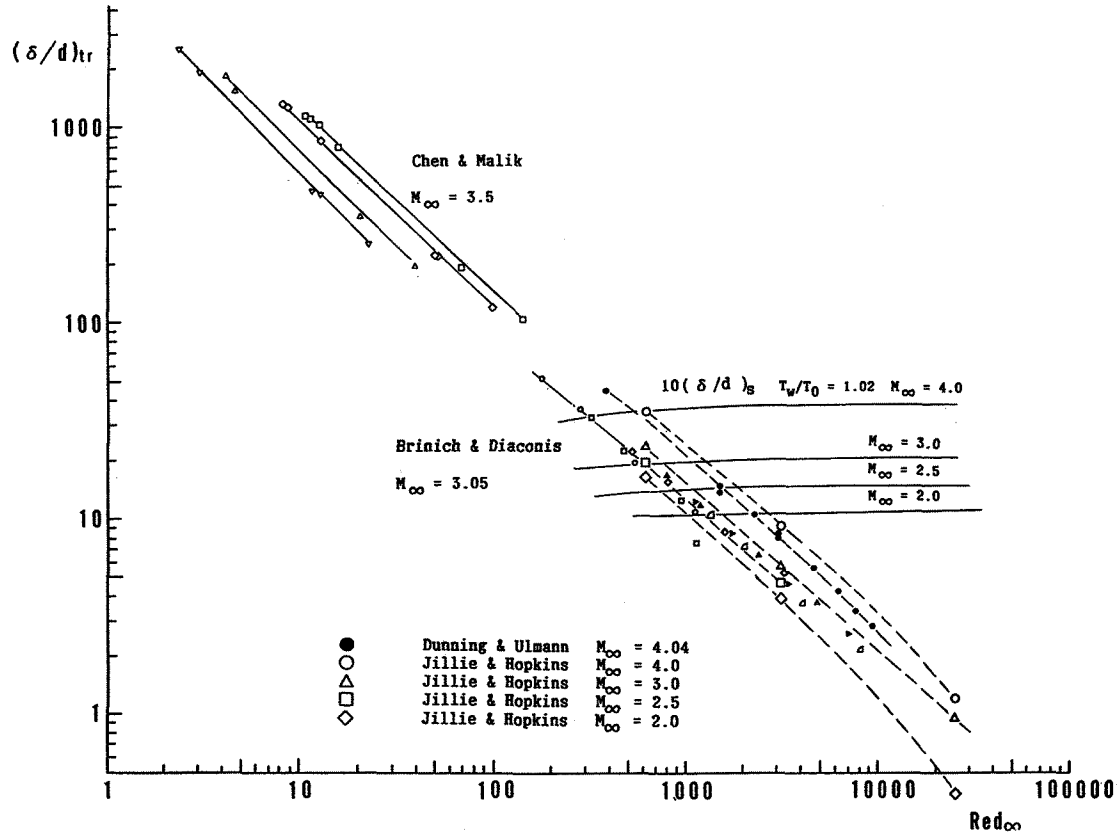

Fig.12 Variation of $(\delta/d)_{tr}$ agaist Red_{∞}

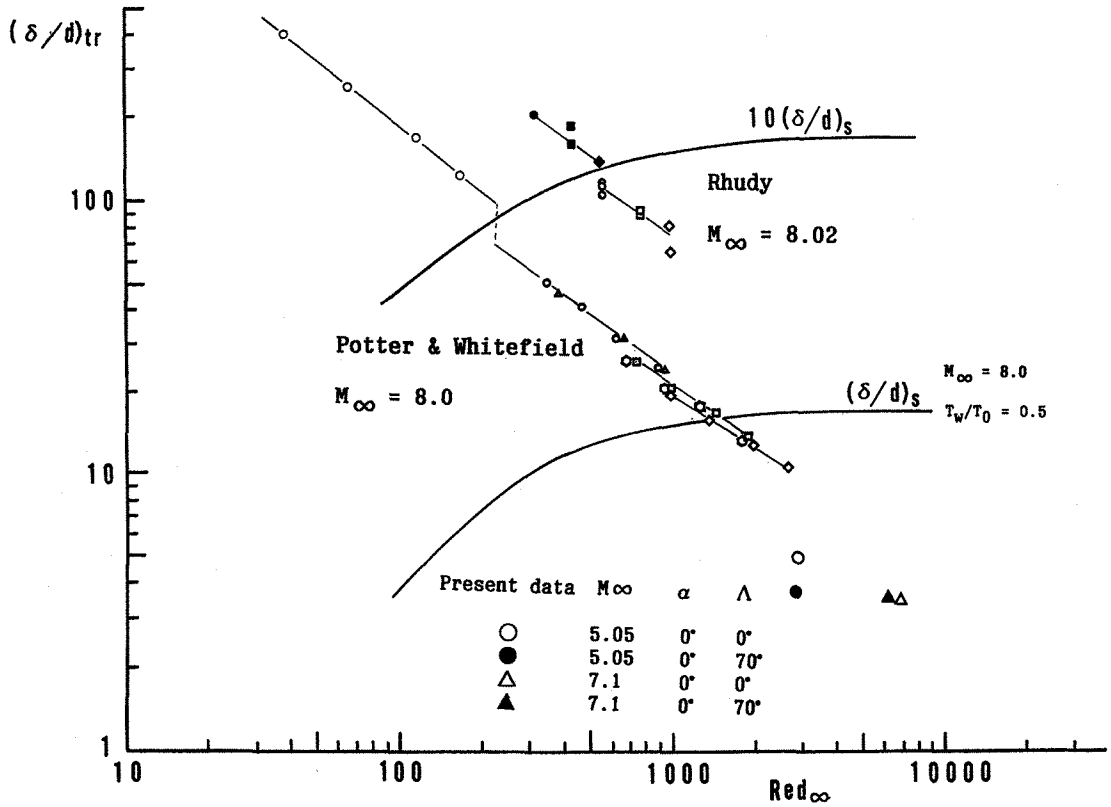

Fig.13 Variation of $(\delta/d)_{tr}$ agaist Red_{∞}